An ab initio structural and spectroscopic study of acetone—An analysis of the far infrared torsional spectra of acetoneh6 and d6

Y. G. Smeyers, M. L. Senent, V. Botella, and D. C. Moule

Additional information on J. Chem. Phys.

An *ab initio* structural and spectroscopic study of acetone—An analysis of the far infrared torsional spectra of acetone-h_6 and -d_6

Y. G. Smeyers, M. L. Senent, and V. Botella
Instituto de Estructura de la Materia, CSIC, c/Serrano, 119, 28006 Madrid, Spain

D. C. Moule
Department of Chemistry, Brock University, St Catharines, Ont., L2S3A1, Canada

The far infrared torsional spectra of acetone $(CH_3)_2CO$ and $(CD_3)_2CO$ have been determined from *ab initio* calculations, and the main features of the experimental data assigned. For this purpose, the potential energy surface for the double methyl rotation was determined with fully relaxed geometry into the RHF and RHF+MP2 approximations using a 6–31G(p,d) basis set. The energy values, as well as the kinetic parameters obtained from the optimized geometry, were fitted to double Fourier expansions as functions of the rotational angles in seven terms. The torsional solutions were developed on the basis of the symmetry eigenvectors of the G_{36} nonrigid group, which factorize the Hamiltonian matrix into 16 boxes. The energy levels and torsional wave functions for each symmetry specie were then obtained diagonalizing each blocks separately. Intensities were obtained from the calculated electric dipole moment variations and the nuclear statistical weights, and were combined with the torsional frequencies to predict the spectra. The calculated band patterns show a multiplet structure and reproduce the main features of the experimental data. The torsional bands of the infrared active ν_{17} mode were found to be clustered into quartets, $(A_1 \rightarrow A_2, G \rightarrow G, E_1 \rightarrow E_1, E_3 \rightarrow E_4)$, for the $v=0 \rightarrow v=1$ fundamental, and $(A_2 \rightarrow A_1, G \rightarrow G, E_1 \rightarrow E_1, E_4 \rightarrow E_3)$ for the $v=1 \rightarrow v=2$ first sequence transitions. The $G \rightarrow G$ transitions were found to be the more intense. The correlation between the calculated and observed spectra allows for an assignment of the major bands.

INTRODUCTION

Acetone is the molecular prototype for the aliphatic ketone series of molecules. In this molecule, the two methyl groups attached to the carbonyl moiety are quite flexible and are able to undergo torsional oscillations. The barriers which restrict the motions are known to be relatively low in this molecule, and thus the two CH_3 groups undergo internal rotation. As the rotors are attached to the same carbon atom, the hydrogen atoms of the methyl groups come into each others proximity and sterically interfere. The low frequency dynamics of coupled methyl rotors has been the subject of an extensive review.[1]

As the torsional motions extend over large amplitudes, it is necessary to regard the complete potential energy surface which is defined by 360° rotations of the two torsional angles. Quantum mechanical molecular techniques have become available which allow the potential energy functions to be obtained with considerable accuracy. The test of the quality of the potential energy functions, of course, must come from the energy levels and torsional wave functions which are derived from the torsional Hamiltonian. A common technique is to solve the internal rotation problem as an expansion in the free rotor basis solutions, and determine the coefficients variationally.[2,3] The symmetry of acetone with two C_{3V} rotors and a C_{2V} frame allows the energy levels to be classified by the irreducible representations of the G_{36} nonrigid group. This high symmetry allows the Hamiltonian matrix to be transformed into 16 smaller blocks corresponding to the 9 representations. As a result,

it is possible to use longer basis sets in the solution of the Hamiltonian with better numerical accuracy. Symmetry also allows for the labeling of the torsional levels, which is useful for the spectroscopic assignment, as well as to deduce selection rules for the transitions. The energy values may be used to predict the frequencies, and the wave functions to calculate the electric dipole moment variations and predict the strengths of the far infrared transitions. The test of the calculation model thus depends on the agreement between the spectra synthesized from *ab initio* molecular calculations and the experimental gas phase spectra.

The microwave spectrum of acetone was first studied by Swalen and Costain[4] and then later by Peters and Dreizler.[5] These authors were able to establish that in the vibrational ground state the methyl groups adopt a conformation in which the in-plane hydrogen atoms eclipse the oxygen. From the satellite patterns in the rotational spectra they were able to determine an effective barrier to internal rotation. At about the same time, Nelson and Pierce[6] observed the spectrum of the deuterated isotopomers and reported an r_S structure. More recently, Iijima[7] determined an average zero-point structure for acetone by combining interatomic distances obtained from electron diffraction with moments of inertia from microwave spectroscopy. The most recent and complete analysis of Vacherand *et al.*[8] covers a wider spectral range and further refines the effective barrier: $V_{\text{eff}}=266.09$ cm^{-1}.

In the rigid equilibrium conformation, acetone pos-

sesses C_{2V} symmetry and the torsional oscillations may be classified into a symmetric and an antisymmetric pair of normal modes. The clockwise–clockwise motion transforms as a rotation about the z (C=O) axis and can be classified as $\nu_{12}(a_2)$. Infrared activity in this mode is forbidden by electric dipole selection rules, although it is allowed by Raman selection rules. The clockwise–counterclockwise combination transforms as an out-of-plane displacement and is allowed in the infrared as an x polarized, type-C transition, $\nu_{17}(b_1)$.

Fateley and Miller[9] first reported the far infrared spectrum of acetone in an early pioneering study. Later at higher resolution Smith, McKenna, and Möller[10] observed bands at 124.5 and 104.5 cm^{-1} which they assigned to e–e and a–a transitions in the $\nu_{17}(b_1)$ mode. The most detailed study of the spectrum to date is that of Groner, Guirgis, and Durig.[11] These authors were able to observe the splittings of the bands into their various torsional components. They assigned the bands at 125.16, 102.92, 92.92/95.95, 89.41, 85.65 cm^{-1} in the $-h_6/-d_6$ isotopomers to the fundamental, first and second sequence transitions in the $\nu_{17}(b_1)$ mode. A Raman spectrum of acetone cooled to liquid nitrogen temperatures has been observed by Harris and Levin.[12] While they were unsuccessful in locating the fundamental modes, they did observe satellites built on the sides of the $\nu_8(a_1)$ in-plane CCC bending fundamental which they attributed to torsion–vibration combination bands. Many studies of the mid-infrared and Raman spectra of acetone have been reported. Noteworthy, are those of Dellepiane and Overend[13] and Hollenstein and Günthard.[14]

Information about the ground state torsional levels has also come from studies of the patterns of hot bands observed in electronic spectra. The transitions which give rise to hot bands in electronic spectra originate from thermally populated vibrational levels of the ground electronic state. Thus they contain information which often complements infrared and Raman data. In a study of the $n \rightarrow 3p_X$ Rydberg transitions of acetone $-h_6$ and $-d_6$ by ultraviolet two-photon resonant multiphoton ionization spectroscopy, Philis, Berman, and Goodman[15] have been able to observe the $\nu_{12}(a_2)$ mode directly as a hot band interval extending back -77 and -55 cm^{-1}, respectively, from the origin bands of the two isotopomers.

There have been a number of theoretical calculations aimed at obtaining barrier maxima and saddle points for acetone.[16] Somewhat fewer studies have been made of the complete torsional potential. The first detailed analysis of the torsional dynamics was made in 1981 by Smeyers and Bellido.[2] In this study, the total energy was mapped out with the CNDO/2 semiempirical method in a 15° grid which was defined by the 360° rotations of the two torsional coordinates. These data points were fitted to a symmetry adapted Fourier expansion in seven terms which defined the potential surface.[17] A semirigid model was used for the kinetic energy in which the frame was fixed at the "standard" geometry. To maintain a sufficient basis length the torsional energy matrix was symmetrized into blocks by the nonrigid operations of the G_{36} point group.[2] Wat-

son[18] has shown that the A_1, A_2, A_3, and A_4 singly degenerate representations of this group correlate to the a_1, b_1, a_2, and b_2 representations of the C_{2V} point group. From a potential surface which was defined by a barrier maximum of 456.7 cm^{-1} and a saddle point of 145.7 cm^{-1} Smeyers and Bellido[2] calculated the $\nu_{17}(b_1)$ and $\nu_{12}(a_2)$ modes to be 91.99 and 67.36 cm^{-1}, respectively, which indicates that the derived potential was too shallow. In later studies Smeyers et al.[19,20] revised the barrier and saddle points upwards to more realistic values by the use of ab initio procedures.

Similar calculations have been reported. Recently, Crighton and Bell[21] were able to calculate values for the two torsional fundamental modes in reasonable agreement to the observed infrared frequencies. They used a semirigid model for acetone in which the frame and the methyl coordinates were fixed at the optimized eclipsed–eclipsed equilibrium geometry. The most recent calculation is that of Ozkabak, Philis, and Goodman.[22,23] These authors used the torsional Hamiltonian of Crighton and Bell and evaluated the energy surface with a variety of different ab initio methods which included corrections for electron correlation. They concluded from a comparison of rigid frame model and the fully relaxed model that a significant flexing of the molecular structure occurs when the methyl groups undergo internal rotation as a result of steric hinderance. Thus the potential surface for the semirigid and the fully relaxed models are quite different. For a 6–31G(d,p) basis they found potential maxima of 1079.04 and 763.92 cm^{-1}, respectively, for the two models.

The aim of this work is to synthesize the far infrared spectra of acetone and its fully deuterated isotopomer from ab initio calculations, and to compare them to the observed spectra. By this technique it should be possible to assign quantum numbers to the higher bands in the spectrum and to determine the effects of nonrigidity on the observed patterns.

THEORY

As a starting point for the analysis of the far infrared spectrum of acetone, we begin with a discussion of the symmetry properties which are brought about by the nonrigid motions of the methyl groups. This is followed by the development of the potential energy function in the dimensions of the two torsional angles. The addition of the kinetic energy leads to the two-dimensional Hamiltonian which is solved variationally for the energy levels and torsional wave functions. Intensities are derived from the transition moments, the level populations and the nuclear statistical weights. The other vibrational modes, such as the bending of the CCC angle or the out-of-plane wagging of the oxygen atom will not be considered explicitly. In particular, the centrifugal distortion of the methyl tops will not be taken into account, since we are only concerned with the lowest torsional levels.

Acetone has a C_{2V} equilibrium structure in the lowest singlet electronic state and the in-plane methyl hydrogen atoms eclipse the oxygen atom, $\theta_1=0°$, $\theta_2=0°$. Figure 1 shows the equilibrium structure of acetone, the symmetry
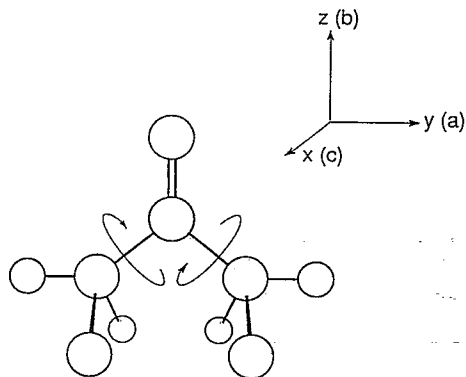
FIG. 1. Structure of acetone, torsional coordinates Θ_1 and Θ_2, Cartesian and principal axes.

axes x, y, z and the principal axes of rotation a, b, c. The directions of rotation of the methyl hydrogen atoms about the C–C bonds are defined in the clockwise sense for both groups. The Hamiltonian operator for a system bearing two equivalent rotors attached to a C_{2V} rigid molecular frame can be written,[24] in the C_3 symmetric and rigid rotor approximation, as

$$\hat{H}(\theta_1,\theta_2) = -\frac{\partial}{\partial\theta_1} B_{11} \frac{\partial}{\partial\theta_1} - \frac{\partial}{\partial\theta_1} B_{12} \frac{\partial}{\partial\theta_2} - \frac{\partial}{\partial\theta_2} B_{21} \frac{\partial}{\partial\theta_1}$$

$$-\frac{\partial}{\partial\theta_2} B_{22} \frac{\partial}{\partial\theta_2} + V(\theta_1,\theta_2), \qquad (1)$$

where B_{11} and B_{22} are the internal rotation constants for the methyl groups and B_{12} the kinetic interaction term. The rotational constants are related to the reduced moments of inertia by the expressions[2,24–26]

$$B_{11} = \frac{\hbar^2}{2} \frac{I_1}{I_1^2 - \Lambda_{12}^2}, \qquad (2)$$

$$B_{12} = \frac{\hbar^2}{2} \frac{\Lambda_{12}}{I_1 I_2 - \Lambda_{12}^2}. \qquad (3)$$

In these expressions I_1 and I_2 are the reduced moments of inertia of the rotors and Λ_{12} is the interaction term

$$\Lambda_{12} = \sum_{i=xyz} A_1 A_2 \lambda_{1i} \lambda_{2i} / M_{ii}, \qquad (4)$$

$$I_1 = A_1 \left(1 - \sum_{i=xyz} A_1 \lambda_{1i}^2 / M_{ii} \right). \qquad (5)$$

A_1 and A_2 are the moments of inertia of the two CH$_3$ groups, λ_{1i} and λ_{2i} the direction cosines between the axes of the methyl group and the ith principal axis with moment M_{ii}.

As is well known, the complete set of the intramolecular conversion operations which commute with the restricted Hamiltonian operator of Eq. (1) define the G_{36} *restricted nonrigid* molecular group.[25] In the case of acetone, in which we have two equivalent rotors of C_{3v} symmetry and a C_{2v} frame, this restricted nonrigid group is expressed as

$$G_{\text{NRG}} = (C_3^{I1} \times C_3^{I2}) \wedge (V^I \times W^I) \sim G_{36}, \qquad (6)$$

which is a group of order 36 isomorphic to the Longuet-Higgins permutations–inversions group,[25,27] G_{36}. The caret means semidirect product. In this expression, the C_3^{I1} and the C_3^{I2} are the threefold rotation subgroups of each rotor, V^I and W^I are, respectively, the double switch and exchange subgroups defined as follows:

$$C_3^{I} = [\hat{E} + \hat{C}_3 + \hat{C}_3^2], \qquad (7)$$

$$V^{I} = [\hat{E} + \hat{V}], \qquad (8)$$

$$W^{I} = [\hat{E} + \hat{W}], \qquad (9)$$

where $\hat{C}_3$, $\hat{V}$, and $\hat{W}$ are the rotation, double switch, and exchange operators, respectively,

$$\hat{V}f(\theta_1,\theta_2) = f(-\theta_1,-\theta_2), \qquad (10)$$

$$\hat{W}f(\theta_1,\theta_2) = f(\theta_2,\theta_1). \qquad (11)$$

The existence of the V operation is related to the presence of symmetry planes in the C_{3v} rotors and the C_{2v} frame. The existence of the W operation is related to the equivalence of the rotors.[28]

The classification of the torsional wave functions by the enabling operations of the G_{36} nonrigid is essential when the symmetries of all of the torsional states are required. For the levels that lie below the barrier, the internal rotation is restricted and resembles a torsional oscillation which is best described by the quantum numbers of the harmonic oscillator. Thus a rigid C_{2V} acetone rather than the fully flexible G_{36} model would be more useful in classifying the quantum levels. In this case, each of the levels of the rigid C_{2V} model contains four microlevels A, E, E, and G for a total degeneracy of nine. The splitting of the levels depends on the degree of restriction of the rotational motion. Thus at the bottom of the well the levels split by torsion may be close together, whereas at the top of the well they will be widely separated. A diagram illustrating the nodal properties of the singly degenerate representations is given in Fig. 2, where the simplest one dimensional representations which were designated A_1, A_2, A_3, and A_4 are plotted as a function of the torsional angles. The diagonal lines represent the nodal properties of the torsional functions. It is the upward sloping line of the A_2 representation which gives the nonrigid properties of $\theta_1 = -\theta_2$, whereas the downward diagonal with $\theta_1 = \theta_2$ correlates to A_3. These two representations then correspond to an out-of-plane displacement in the x direction and to a rotation about the z axis. They transform, respectively, as a_2 and b_1. The correlations between the G_{36} and the C_{2V} groups are given in Table I.[25]
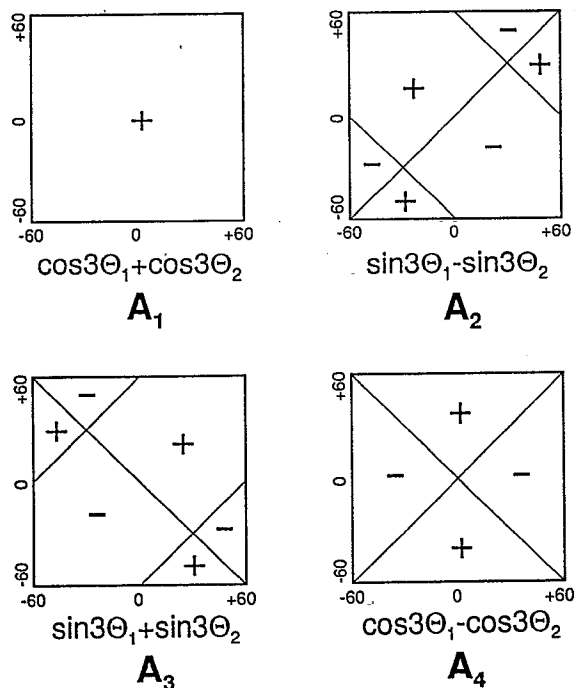
FIG. 2. Nodal properties of the A_1, A_2, A_3, and A_4 nondegenerate torsional wave functions.

The potential energy function for internal rotation in planar acetone can be developed in terms of the A_1 symmetry basis vectors

$$V(\theta_1,\theta_2) = \sum_{L>K} \sum_K (A_{KL}^{cc}[\cos 3K\theta_1 \cos 3L\theta_2$$

$$+\cos 3L\theta_1 \cos 3K\theta_2] + A_{KL}^{ss}[\sin 3K\theta_1 \sin 3L\theta_2$$

$$+\sin 3L\theta_1 \sin 3K\theta_2]) + \sum_L [A_{LL}^{cc} \cos 3L\theta_1$$

$$\times\cos 3L\theta_2 + A_{LL}^{ss} \sin 3L\theta_1 \sin 3L\theta_2]. \qquad (12)$$

Since the molecular geometry changes slightly during the optimization process, the B_{11} and B_{12} kinetic parameters (2) and (3) are also dependent on the torsional angles. They can be developed in terms of the A_1 vectors as the potential (12).

The Schrödinger equation for the two coupled rotor problem, Eq. (1) was solved variationally. The solutions were expanded in terms of a set of the free double rotor basis functions

$$\Phi = \sum_I \sum_J [C_{IJ}^{cc} \cos I\theta_1 \cos J\theta_2 + C_{IJ}^{cs} \cos I\theta_1 \sin J\theta_2$$

$$+C_{IJ}^{sc} \sin I\theta_1 \cos J\theta_2 + C_{IJ}^{ss} \sin I\theta_1 \sin J\theta_2] \qquad (13)$$

and the coefficients determined by diagonalizing the corresponding Hamiltonian matrix.

The oscillator strength was calculated from the approximate relationship[29]

$$f_{fi} = \frac{g}{3B} (E_f - E_i)(C_f - C_i) \left\langle \psi_f \left| \frac{\mu(\theta_1,\theta_2)}{\mathrm{Re}} \right| \psi_i \right\rangle^2 . \qquad (14)$$

In this expression E_i and E_f are the energies and ψ_i and ψ_f are the wave functions of the initial and final states connected by the transition. The coefficients C_i and C_f are the populations of the two states which may be derived from Boltzmann statistics. R is the average distance between the positions of the hydrogen atoms and the methyl rotation axis, e is the elemental electron charge, g_{ii} the nuclear statistical weight, and B the average of the internal rotation constants.

$\mu(\theta_1,\theta_2)$, the dipole moment, was resolved into the three components along the x, y, and z directions, which can be classified according to the A_2, A_4, and A_1 representations of the G_{36} group, as shown in Table I. Each of these components can be developed in terms of the corresponding symmetry eigenvectors[2]

$$\mu_x(\theta_1,\theta_2) = \sum_L \sum_K \mu_{KL_x}^{cc}[\cos 3K\theta_1 \sin 3L\theta_2$$

$$-\sin 3L\theta_1 \cos 3K\theta_2], \qquad (15)$$

$$\mu_y(\theta_1,\theta_2) = \sum_{L>K} \sum_K (\mu_{KL_y}^{cc}[\cos 3K\theta_1 \cos 3L\theta_2$$

$$-\cos 3L\theta_1 \cos 3K\theta_2]$$

$$+\mu_{KL_y}^{ss}[\sin 3K\theta_1 \sin 3L\theta_2$$

$$-\sin 3L\theta_1 \sin 3K\theta_2]), \qquad (16)$$

TABLE I. The correlation of the singly degenerate representations of the G_{36} nonrigid group with the representation of the C_{2V} point group.

C_{2V}	G_{36}	$\hat{E}$ $\hat{E}$	$\hat{C}_2$ $\hat{W}$	$\hat{\sigma}_{XZ}$ $\hat{W}\hat{V}$	$\hat{\sigma}_{YZ}$ $\hat{V}$	Transformation properties		
						C_{2V}	G_{36}	U
a_1	A_1	1	1	1	1	$\cos 2\Theta$	$\cos 3\Theta_1 + \cos 3\Theta_2$	T_Z
a_2	A_3	1	1	-1	-1	$\sin 2\Theta$	$\sin 3\Theta_1 + \sin 3\Theta_2$	R_Z
b_1	A_2	1	-1	1	-1	$\cos \Theta$	$\sin 3\Theta_1 - \sin 3\Theta_2$	T_X
b_2	A_4	1	-1	-1	1	$\sin \Theta$	$\cos 3\Theta_1 + \cos 3\Theta_2$	T_Y

TABLE II. Selection rules for the far infrared transitions in acetone.

T_Z (A_1)	T_Y (A_4)	T_X (A_2)
$A_1 \leftrightarrow A_1$	$A_1 \leftrightarrow A_4$	$A_1 \leftrightarrow A_2$
$A_2 \leftrightarrow A_2$	$A_2 \leftrightarrow A_3$	$A_3 \leftrightarrow A_4$
$A_3 \leftrightarrow A_3$		
$A_4 \leftrightarrow A_4$		
$E_1 \leftrightarrow E_1$	$E_1 \leftrightarrow E_2$	$E_1 \leftrightarrow E_1$
$E_2 \leftrightarrow E_2$	$E_3 \leftrightarrow E_4$	$E_2 \leftrightarrow E_2$
$E_3 \leftrightarrow E_3$		$E_3 \leftrightarrow E_4$
$E_4 \leftrightarrow E_4$		
$G \leftrightarrow G$	$G \leftrightarrow G$	$G \leftrightarrow G$

TABLE III. The potential energy of acetone at different conformations relative to the eclipsed–eclipsed conformation in the RHF and MP2/RHF approximations.[a,b]

No.	Θ_1	Θ_2	RHF	MP2/RHF
(A)	0.0	0.0	0.00[c]	0.00[d]
(B)	60.0	60.0	763.92	793.62
(C)	0.0	60.0	246.85	267.07
(D)	30.0	30.0	229.71	252.34
(E)	30.0	90.0	397.52	412.84
(F)	0.0	30.0	120.82	129.31
(G)	30.0	60.0	508.94	535.53

[a]Energy in cm^{-1}.
[b]Basis set employed: 6–31G(d,p).
[c]Total energy = −191.972 072 hartrees.
[d]Total energy = −192.589 477 hartrees.

$$
\mu_z(\theta_1,\theta_2) = \sum_{L>K} \sum_K (\mu_{KL_z}^{cc}[\cos 3K\theta_1 \cos 3L\theta_2
$$

$$
+ \cos 3L\theta_1 \cos 3K\theta_2] + \mu_{KL_z}^{ss}
$$

$$
\times [\sin 3K\theta_1 \sin 3L\theta_2 + \sin 3L\theta_1 \sin 3K\theta_2]]
$$

$$
+ \sum_L [\mu_{LL_z}^{cc} \cos 3L\theta_1 \cos 3L\theta_2
$$

$$
+ \mu_{LL_z}^{ss} \sin 3L\theta_1 \sin 3L\theta_2]. \tag{17}
$$

From the G_{36} character table,[2,25] selection rules for the infrared transitions are easily deduced. They are given in Table II. The allowed transitions which give rise to C type bands (directed out of the molecular plane, x polarized) of interest here are $A_1 \rightarrow A_2$, $A_3 \rightarrow A_4$, $E_1 \rightarrow E_1$, $E_2 \rightarrow E_2$ $E_3 \rightarrow E_4$, and $G \rightarrow G$. In addition, because of the A_2 symmetry properties of the x component of the dipole moment, the allowed transitions between the degenerate states are restricted to pairs of components which are symmetric and antisymmetric with respect to the exchange and double switch operations.

The wave funtion that describes the motion of a set of particles, Ψ_N, has to be completely symmetric or antisymmetric with respect to the interchange of the position and spin coordinates of all identical particles.[30] In the case of the internal rotation, the overall rotation and the spin nuclear functions Ψ_R and Ψ_S have to be also considered

$$
\Psi_N = \Psi_V \Psi_R \Psi_S, \tag{18}
$$

where Ψ_V is the torsional wave function.

The symmetry properties of the torsional wave functions of acetone are given by the nonrigid group G_{36}.[6] In the case of the C band of the FIR spectrum, the overall rotational function can be only either completely symmetric or completely antisymmetric. Furthermore, since this study does not treat the individual rotational structures, but rather the overall torsional contours, only an average weight has to be retained. As a result, the Ψ_R has to be only completely symmetric or completely antisymmetric.

When the two possible spin coordinates of the protons, or the three possible ones of the deuteriums are taken into account, the spin nuclear wave functions will exhibit degeneracies of orders $2^6 = 64$ or $3^6 = 729$, respectively. All these functions can be classified according to the irreducible representations of the G_{18} nonrigid group, a set anal-

ogous to the G_{36} group, in which the double switch operation, V, has been deleted.[31] The spin functions behave indeed as vectors and no symmetry plane can be retained.

The degeneracies, g_{ii}, of Eq. (15), or nuclear statistical weights, are then given, for each torsional symmetry, i, by the weights of the completely symmetric (and antisymmetric) components in all the possible direct products $\Psi_V \times \Psi_S$. In the acetone h_6 case, we found 16, 32, 8, and 8 completely symmetric (or antisymmetric) products $\Psi_V \Psi_S$ for the A, G, E_1 (or E_2) and E_3 (or E_4) torsional symmetries. In the acetone d_6 case, we found 121, 352, 128, and 128 of such products.[4]

CALCULATIONS AND RESULTS

The starting point for the interpretation of the far infrared spectrum was a calculation of the frequencies and the strengths of the torsional transitions. For this purpose, *ab initio* calculations with full geometry optimization were performed at a restricted Hartree–Fock level (RHF). In these calculations, a 6–31G(d,p) basis set was used. In addition, the electronic correlation was also partially taken into account resorting to Möller–Plesset perturbation calculations up to the second order considering all the electrons (MP2/RHF). The computations were performed with the GAUSSIAN 86 program on a CRAY X-MP.

To establish the potential energy map, the total molecular energy was calculated at seven selected values of the torsional angles.[17] The following structural configurations were used: A($\Theta_1 = 0°$, $\Theta_2 = 0°$, the eclipsed–eclipsed conformation), B($\Theta_1 = 60°$, $\Theta_2 = 60°$, staggered–staggered conformation), C($\Theta_1 = 0°$, $\Theta_2 = 60°$, saddle point), D($\Theta_1 = 30°$, $\Theta_2 = 30°$, upwards rising diagonal), E($\Theta_1 = 30°$, $\Theta_2 = 90°$, downwards falling diagonal), F($\Theta_1 = 0°$, $\Theta_2 = 30°$), G($\Theta_1 = 30°$, $\Theta_2 = 60°$). Because of the G_{36} symmetry, these data points were sufficient to establish a net of points in a grid of 30° intervals on the potential energy surface defined by the Θ_1 and Θ_2. In each of these calculations, a complete optimization of the geometrical parameters was carried out, except for the heavy atoms which were restricted to be in the molecular plane.

The energies relative to the most stable conformer (A) are given in Table III for both RHF and MP2/RHF mod-
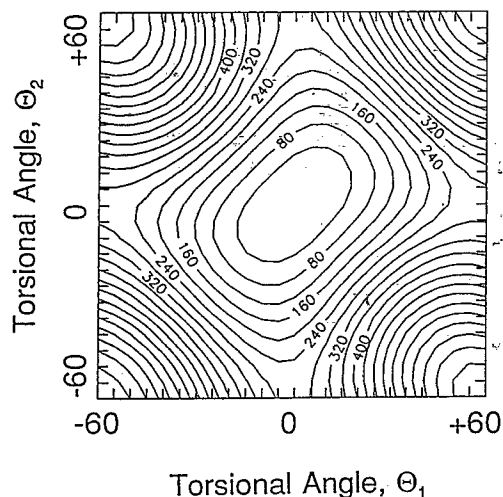
FIG. 3. Contour plot of the potential energy surface. The contour lines are 40 cm^{-1} apart.

els. The RHF calculation generates an energy difference relative to the staggered–staggered conformation (B) of 763.92 cm^{-1} which is to be compared to the value corrected for configuration interaction of 793.62 cm^{-1}. The saddle point conformation (C) at 246.85 cm^{-1} (MP2 267.07 cm^{-1}) is considerably smaller than one-half the barrier maximum at (B) which demonstrates that the rotor coupling is important. Figure 3 shows a plot of a 120° ×120° segment of the "egg box" potential energy surface. It is clear that the walls of the potential surface are steeper in the direction where the methyl groups rotate in the opposite senses, (A_2) b_1, than they are in the direction where the rotors move in the same direction. Compare point (D) at 229.71 cm^{-1} (MP2=252.34 cm^{-1}) with point (E) at 397.52 cm^{-1} (MP2=412.84 cm^{-1}). Thus it would be anticipated that the frequency of the gearing A_2 (b_1) mode would be higher than the antigearing A_3 (a_2) mode (see Fig. 4).
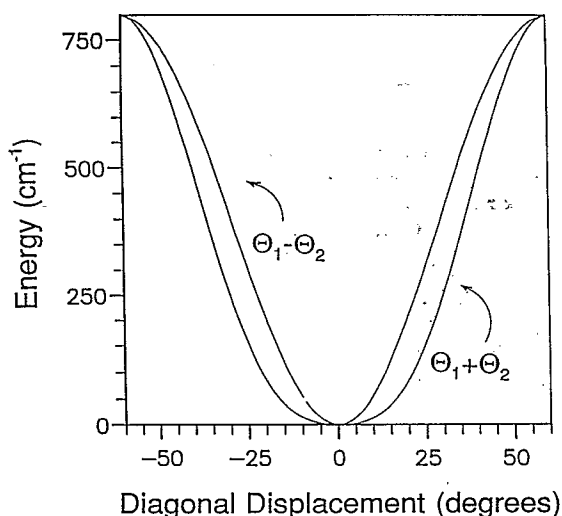
The geometries obtained from the MP2/RHF calculations are given in Table IV. It is instructive to compare the bond lengths and bond angles of the conformers (A) and (B) which have C_{2V} symmetry. While the C=O bond length does not change very much as the result of a rotation of Θ_1 and Θ_2 by 60°: 1.2257 to 1.2256 Å, substantial changes occur in the methyl end of the molecule. For example, on going from (A) to (B) the C–C bond length increases from 1.5112 to 1.5159 Å, the CCC angle opens from 116.38° to 119.44°, and the CCH$_1$ from 109.59° to 113.15°. These changes in structure operate in the direction relieving the steric repulsion between the inner in-plane hydrogens which crowd together in the staggered–staggered conformation (B). This adjustment of the bond lengths and bond angles has the net effect of increasing the H$_1$–H$_4$ distance by 0.24 Å. Philis, Berman, and Goodman[15] have shown that this structural relaxation results in a 293.21 cm^{-1} reduction in total energy.

The seven Fourier expansion coefficients of Eq. (12) given in Table V were determined from the data points of Table III. The global coupling between the rotors is described mainly by the $\cos(3\Theta_1)\cos(3\Theta_2)$ and the gearing effect by the $\sin(3\Theta_1)\sin(3\Theta_2)$ terms.[17]

The B_{ij} kinetic parameters for each of the seven conformations were calculated from the structural data of Table IV, and are given in Table VI. The Fourier expansions determined from these values are given in Table VII. The small variation observed between the extremes in the constants, $B_{11}(\Theta_1=0°,\Theta_2=0°)=5.686\,323$ cm^{-1} and $B_{11}(\Theta_1=60°,\Theta_2=60°)=5.677\,853$ cm^{-1} indicates that the kinetic energy is almost insensitive to the variation of the torsional coordinates. The three C–H bonds of the methyl group can be regarded as a propeller which spins around the C–C bond. If the blades on the propeller are finely balanced, then the center of mass of the system will not change too much and the propeller will rotate with roughly constant moment of inertia.

The torsional Schrödinger equation corresponding to the Hamiltonian operator (1) was solved variationally by using the RHF or MP2/RHF potentials. For this purpose, the torsional solutions were developed in terms of the symmetry eigenvectors,[2] which factorize the Hamiltonian matrix in blocks. Each methyl group was described by 31 basis functions to give an overall order of 961 for the Hamiltonian matrix, which is factorized into the 16 blocks corresponding to the representations of the G_{36} symmetry group $A_1(36)$, $A_2(30)$, $A_3(30)$, $A_4(25)$, $G(4×110)$, $E_1(2×55)$, $E_2(2×45)$, $E_3(2×55)$, $E_4(2×45)$. This previous symmetry factorization was found to reduce the computational time by a factor of 250. On the other hand, the adequacy of the basis length employed was checked by using different basis lengths up to reach self-consistency in the energy values of the lowest levels under 500 cm^{-1}, which are well above the saddle point.

In the lower regions of the potential, where the internal rotation is not entirely free, the levels can be described by the $v(b_1)$ and $v(a_2)$ quantum numbers of the C_{2V} point group. As the potential surface has nine minima for every

FIG. 4. The potential energy curves in the b_1 and a_2 directions.

TABLE IV. Acetone MP2/RHF optimized geometry parameters for selected torsional conformers (in Angstroms and degrees).[a,b]

Θ_1–Θ_2	0–0	0–30	30–30	0–60	30–60	60–60	90–30
Bond lengths							
C1=O	1.2257	1.2256	1.2254	1.2254	1.2255	1.2256	1.2258
C1–C2	1.5112	1.5199	1.5120	1.5085	1.5160	1.5159	1.5135
C1–C3	1.5112	1.5132	1.5120	1.5159	1.5123	1.5159	1.5135
C2–H1	1.0847	1.0847	1.0902	1.0847	1.0856	1.0853	1.0904
C2–H2	1.0892	1.0891	1.0871	1.0896	1.0877	1.0879	1.0862
C2–H3	1.0892	1.0897	1.0856	1.0896	1.0879	1.0879	1.0856
C3–H4	1.0847	1.0901	1.0902	1.0862	1.0905	1.0853	1.0904
C3–H5	1.0892	1.0869	1.0871	1.0877	1.0863	1.0879	1.0862
C3–H6	1.0892	1.0855	1.0856	1.0877	1.0857	1.0879	1.0856
Bond angles							
C2–C1=O	121.81	121.92	121.39	122.08	120.44	120.28	120.99
C3–C1=O	121.81	121.26	121.39	120.67	121.17	120.28	120.99
C2–C1–C3	116.38	116.82	117.21	117.26	118.38	119.44	118.03
C1–C2–H1	109.59	109.67	108.53	109.79	113.04	113.15	109.03
C1–C2–H2	110.19	109.93	112.19	109.97	109.11	108.75	112.36
C1–C2–H3	110.19	110.24	109.38	109.97	108.48	108.75	108.92
C1–C3–H4	109.59	108.82	108.53	112.81	108.71	113.15	109.03
C1–C3–H5	110.19	112.12	112.19	108.87	112.39	108.75	112.36
C1–C3–H6	110.19	109.32	109.38	108.87	109.13	108.75	108.92
H1–C2–H2	109.79	109.77	108.30	109.95	109.52	109.35	108.28
H2–C2–H3	107.24	107.22	110.41	107.17	107.38	107.32	110.40
H4–C3–H5	109.79	108.08	108.30	109.33	108.34	109.35	108.28
H5–C3–H6	107.24	110.37	110.41	107.49	110.44	107.32	110.40

[a]For RHF values see Ref. 32.
[b]Basis set employed: 6–31G(d,p).

full rotation of the methyl groups, the zero point level A_1 $v(b_1)=0$, $v'(a_2)=0$, has nine microstates.

From Table VIII(A), these microstates can be identified as belonging to the A_1, G, E_1, and E_3 states. In the case of the MP2/RHF calculations with B_{ij} variable, these lie at 108.867, 108.909, 109.113, and 109.108 cm^{-1} relative to the bottom of the well. Thus the vibrational zero point level of acetone contains four sublevels whose separations depend mainly on the magnitude of the barriers to internal rotation. Since the potential energy surface calculated with MP2/RHF approximation is somewhat sharper, the torsional levels obtained in the RHF approximation lie somewhat lower: 105.294, 105.357, 105.592, 105.577 cm^{-1}.

Table VIII(A) also shows the energy level positions for acetone which have not been corrected for the variation in the kinetic energy. For example, the lowest level A_1 in the MP2/RHF calculations lies at 108.902 cm^{-1}, whereas when corrected for variable kinetic energy it lies at 108.867

cm^{-1}. This 0.035 cm^{-1} energy correction could be anticipated from Table VI. The coefficients of the Fourier expansions in $B_{11}(\Theta_1,\Theta_2)$ and $B_{12}(\Theta_1,\Theta_2)$ show a constant term which is about 1000 times larger than the terms in the Θ_1 and Θ_2 variables. The conclusion follows that the hydrogen atoms of the methyl groups rotate about the C–C bond without appreciable shift of the center of mass. That is, the methyl hydrogen atoms move very approximately in a circular orbital motion.

The rigid–nonrigid symmetry correlation of Table I, a_1, a_2, b_1, and b_2 with A_1, A_3, A_2, and A_4, allows the energy levels to be labeled by the v and v', the quantum numbers for small amplitude oscillation. Thus the second set of levels in the MP2/RHF torsional manifold at 193.001, 192.471, 191.998, and 192.013 cm^{-1} is identified with the antigearing $\nu_{12}(a_2)$ mode, $v=1$, $v'=0$. The third set at

TABLE V. Calculated expansion coefficients for the potential energy in acetone.[a]

	RHF	MP2/RHF
A_{00}^{cc}	314.445 38	332.342 50
A_{10}^{cc}	−192.520 00	−200.757 50
A_{11}^{cc}	67.555 00	64.870 00
A_{20}^{cc}	0.197 12	−0.162 50
A_{21}^{cc}	1.540 00	2.352 50
A_{22}^{cc}	−0.434 62	−0.077 50
A_{11}^{ss}	−83.906 50	−80.077 50

[a]Energy in cm^{-1}.
[b]Basis set employed: 6–31G(d,p).

TABLE VI. The internal rotation constants B_1 and B_{12} for selected conformations[a] of acetone, MP2/RHF.[b,c]

Θ_1–Θ_2	$(CH_3)_2CO$		$(CD_3)_2CO$	
	$B_1=B_2$	B_{12}	$B_1=B_2$	B_{12}
0–0	5.686 323	−0.183 921	2.966 994	−0.174 832
0–30	5.682 335	−0.189 173	2.968 222	−0.179 975
30–30	5.696 429	−0.194 272	2.971 012	−0.184 908
0–60	5.677 853	−0.194 010	2.966 471	−0.184 615
30–60	5.709 745	−0.200 358	2.988 045	−0.189 172
60–60	5.724 428	−0.217 062	2.996 191	−0.206 177
30–90	5.705 868	−0.202 101	2.983 628	−0.192 193

[a]Values in cm^{-1}.
[b]For RHF values see Ref. 32.
[c]Basis set employed: 6–31G(d,p).

TABLE VII. Expansion coefficients[a] for the kinetic energy.[b,c]

| | (CH$_3$)$_2$CO | | (CD$_3$)$_2$CO | |
	$B_1 = B_2$	B_{12}	$B_1 = B_2$	B_{12}
B^{cc}_{00}	5.700 658 8	−0.196 242 06	2.979 697 6	−0.186 314 31
B^{cc}_{10}	−0.009 252 4	0.006 938 88	−0.007 346 0	0.006 217 38
B^{cc}_{11}	0.004 576 8	−0.003 240 75	0.002 157 5	−0.002 944 75
B^{cc}_{20}	−0.000 087 4	0.000 233 94	−0.000 528 8	0.000 247 69
B^{cc}_{21}	−0.000 273 9	0.001 346 38	0.000 046 8	0.001 618 88
B^{cc}_{22}	0.000 314 8	−0.001 476 56	−0.001 320 3	−0.001 740 81
B^{cs}_{11}	−0.004 719 5	0.003 914 50	−0.006 308 0	0.003 642 50

[a]In cm^{-1}.
[b]Basis set employed: 6–31G(d,p).
[c]For RHF values see Ref. 32.

239.540, 238.356, 237.602, and 237.583 cm^{-1} then is associated with the gearing mode $\nu_{17}(b_1)$, $v=0$, $v'=1$. The A_4 level, b_2, $v=1$, $v'=1$, is obtained as a combination of the ν_{12} and ν_{17} modes.

To obtain the band intensities, the oscillator strength (14) was employed. This requires the expansion of the dipole moment components as Fourier series, Eqs. (15), (16), and (17). Since the calculations developed here will be limited to the C band, only the x component will be considered next. This was accomplished by the dipole moment data of Table IX and gave the coefficients $\mu^{cs}_{01}=0.055\ 675$, $\mu^{cs}_{11}=-0.000\ 80$, and $\mu^{sc}_{12}=0.002\ 975$ D. In Fig. 5, we represent the dipole component variations as a function of the rotational angles. It is clear that the negative and positive regions of the dipole moment map correlate to the corresponding region of the A_2 torsional wave function of Fig. 2. Finally, the far infrared spectra for (CH$_3$)$_2$CO and (CD$_3$)$_2$CO are synthesized in Tables X(A) and X(B) which collect together the band frequencies and intensity data.
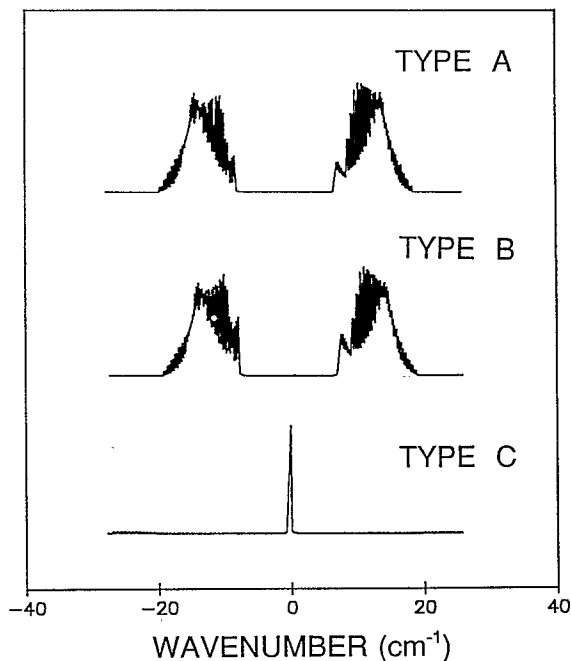
FIG. 6. The A-, B-, and C-type contour bands. Notice that the vertical axis is contracted in the case of the C-type band.

ASSIGNMENT

The far infrared spectra of acetone and acetone-d_6 were recorded by Groner, Guirgis, and Durig.[11] The spectra are complex and consist of a series of linelike features which are superimposed on a strongly absorbing background. It is possible to attribute these absorption lines to the central Q branches of type-C transitions (directed out of the molecular plane). To confirm this assignment, the overall rotational contours of the bands were simulated in the rigid rotor approximation for the $v=0(A_1) \rightarrow v=1(A_2)$ torsional component of the ν_{17} mode. The rotational constants for the two combining states were calculated from the structural data of Table IV. For this purpose, the moments of inertia for the seven conformations were fitted to a double Fourier expansion in Θ_1 and Θ_2 to yield $I_A(\Theta_1,\Theta_2)$, $I_B(\Theta_1,\Theta_2)$, and $I_C(\Theta_1,\Theta_2)$. Expectation values for the moments of inertia were evaluated from the torsional wave functions of the two levels Ψ_{A1}, Ψ_{A2} through the relationships $\langle\Psi_{A1}|I_A(\Theta_1,\Theta_2)^{-1}|\Psi_{A1}\rangle$, $\langle\Psi_{A1}|I_B(\Theta_1,\Theta_2)^{-1}|\Psi_{A1}\rangle$, and $\langle\Psi_{A1}|I_C(\Theta_1,\Theta_2)^{-1}|\Psi_{A1}\rangle$ to give $A''_{A1} = 0.336\ 391$, $B''_{A1} = 0.285\ 143$, $C''_{A1} = 0.163\ 610$, $A'_{A2} = 0.337\ 502$, $B'_{A2} = 0.284\ 117$, and $C'_{A2} = 0.163\ 512$ cm^{-1}. Using these expectation values the locations of the lowest levels of the experimental microwave spectrum were well reproduced.[4] These values were then inserted into a rigid rotor band contour program[32] and the overall contours of the A-, B-, and C-type transitions simulated for $J_{MAX}=49$ and $K_{MAX}=30$.

Acetone is a near oblate symmetric top with the top axis perpendicular to the molecular plane. The type-A and -B transitions lie in the molecular plane and, as illustrated in Fig. 6, they give rise to similar smooth bands which have
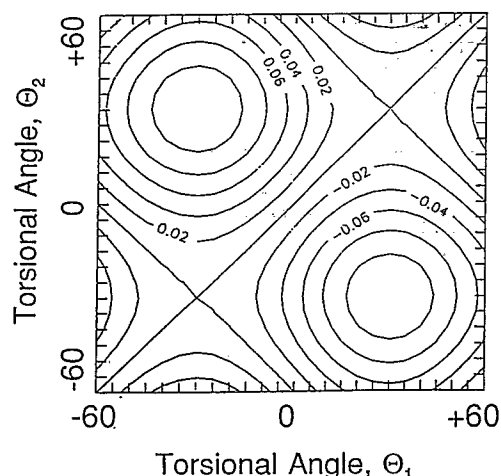

FIG. 5. The plot of the component of the dipole moment $\mu_x(\Theta_1,\Theta_2)$ in the out-of-plane x direction. The intervals are at 0.02 D.

TABLE VIII. (A) Acetone-h_6 energy levels. (B) Acetone-d_2 energy levels.[a,b]

(A) Acetone-h_6

(v,v')	C_{2V}	G_{36}	Constant kinetic energy parameters		Variable kinetic energy parameters	
			MP2/RHF	RHF	MP2/RHF	RHF
(0,0)	a_1	A_1	108.909	105.340	108.867	105.294
		G	108.972	105.426	108.909	105.357
		E_1	109.036	105.512	109.113	105.592
		E_3	109.035	105.511	109.108	105.577
(1,0)	a_2	A_3	192.996	184.790	193.001	184.720
		G	192.447	184.103	192.471	184.076
		E_2	191.919	183.449	191.998	183.463
		E_3	191.921	183.453	192.013	183.486
(0,1)	b_1	A_2	239.807	234.424	239.540	234.214
		G	238.623	232.832	238.356	232.615
		E_1	237.432	231.236	237.602	231.444
		E_4	237.427	231.230	237.583	231.419
(2,0)	a_1	A_1	282.263	270.037	282.283	270.017
		G	284.050	271.930	284.057	271.908
		E_1	288.125	276.768	288.258	276.871
		E_3	287.970	276.507	288.106	276.601
(1,1)	b_2	A_4	292.088	279.612	291.983	279.478
		G	298.736	287.381	298.631	287.252
		E_2	303.360	292.488	303.393	292.468
		E_4	303.670	293.030	303.718	293.045
(0,2)	a_1	A_1	350.123	339.253	349.860	339.052
		G	350.416	338.192	350.229	338.052
		E_1	351.168	338.730	351.301	338.888
		E_3	349.953	336.752	350.076	336.851

(B) Acetone-d_6

(v,v')	C_{2V}	G_{36}	Constant kinetic energy parameters		Variable kinetic energy parameters	
			MP2/RHF	RHF	MP2/RHF	RHF
(0,0)	a_1	A_1	79.182	76.608	79.110	76.552
		G	79.184	76.611	79.097	76.540
		E_1	79.186	76.613	79.290	76.737
		E_3	79.186	76.614	79.284	76.733
(1,0)	a_2	A_3	137.316	130.983	137.285	130.994
		G	137.294	130.952	137.280	130.981
		E_2	137.373	130.921	137.365	131.062
		E_3	137.273	130.921	137.374	131.071
(0,1)	b_1	A_2	178.099	174.252	177.758	173.953
		G	178.043	174.162	177.686	173.847
		E_1	177.986	174.072	178.222	174.319
		E_4	177.987	174.072	178.210	174.308
(2,0)	a_1	A_1	203.653	194.501	203.612	194.558
		G	203.810	194.708	203.816	194.795
		E_1	203.974	194.925	204.139	195.179
		E_3	203.973	194.923	204.139	195.171
(1,1)	b_2	A_4	224.837	216.503	224.587	216.332
		G	225.330	217.187	225.048	216.989
		E_2	225.826	217.877	225.858	217.968
		E_4	225.828	217.881	225.874	217.984
(0,2)	a_1	A_1	270.496	263.533	270.061	263.153
		G	270.851	264.832	270.478	260.472
		E_1	271.677	264.492	271.968	264.745
		E_3	270.436	266.300	270.663	266.624

[a]In cm^{-1}.
[b]Basis set employed: 6–31G(d,p).

TABLE IX. Components of the dipole moment of acetone.[a,b]

Θ_1	Θ_2	μ_y	μ_z	μ_x
0.0	0.0	0.0	3.1407	0.0
0.0	30.0	−0.0011	3.1194	−0.0519
30.0	30.0	0.0	3.0943	0.0
0.0	60.0	0.0757	3.0929	0.0
30.0	60.0	0.0100	3.0498	0.0535
60.0	60.0	0.0	3.0072	0.0
30.0	90.0	0.0	3.0757	0.1173

[a]Approximation: RHF, basis set: 6–31G (d,p).
[b]Values in Debye units.

(a)

(b)

FIG. 7. (a) Observed and calculated far infrared spectra of acetone-h_6. (b) Observed and calculated far infrared spectra of acetone-d_6.

distinct P and R branches. On the contrary, the type-C transitions, which are directed along the top axis, are characterized by a strong central Q branch. Thus the observed linelike features can be attributed to the type-C bands, which stand out as clearly defined peaks on the strongly absorbing background continuum due to the P and R branches.

Theoretical spectra were synthesized for acetone-h_6 and -d_6 from the frequency and intensity data of Tables X(A) and X(B) and were plotted by simulating the contours of the bands with a Lorentzian broadening function with a line width of 0.5 cm^{-1}. Figures 7(a) and 7(b) show the results and compare the calculated spectra with the observed far infrared spectra which were reproduced from Fig. 1 of Ref. 11. A correlation between the two spectra allows for an assignment of the major bands.[33]

For acetone-h_6, the fundamental frequency for the methyl rotation clockwise–counterclockwise ν_{17} torsion mode $v=0(G)\to v=1(G)$ is calculated at the level MP2/RHF to lie at 129.447 cm^{-1} as the strongest band in the spectrum, intensity, 0.9044×10^{-4}. The assignment of this transition to the peak at 124.61 cm^{-1} follows without difficulty. The second strongest peak is observed in the spectrum at 104.20 cm^{-1} and is assigned on the basis of its calculated intensity, 0.3271×10^{-4}, to the first sequence transition $v=1(G)\to v=2(G)$. The calculated position is 111.873 cm^{-1}. The second sequence transition in the spectrum $v=2(G)\to v=3(G)$, is calculated to lie at 139.143 cm^{-1}.

The major bands were observed to have a multiplet structure which results from the transitions which occur between the torsional microstates associated with each level. The band which is assigned to the ν_{17} fundamental $v=0\to v=1$ is calculated to be complex and to result from the transitions: $A_1\to A_2$, 130.673 cm^{-1} (0.4705×10^{-4}); $G\to G$, 129.447 cm^{-1} (0.9044×10^{-4}); $E_1\to E_1$, 128.489 cm^{-1} (0.2185×10^{-4}); $E_3\to E_4$, 128.474 cm^{-1} (0.2184×10^{-4}). Thus the ν_{17} fundamental would consist of four bands which are clustered within a frequency interval of 2.20 cm^{-1}. The prominent band observed at 124.61 cm^{-1} is somewhat broader than would be expected for a single transition. Arranged on either side of this central peak are a partially resolved satellite at 125.16 cm^{-1} and a shoulder at 123.90 cm^{-1}. We assign the high frequency member to the $A_1\to A_2$ transition, and the low frequency shoulder to the combination $E_1\to E_1$ and $E_3\to E_4$.

The band which is assigned to the first sequence is

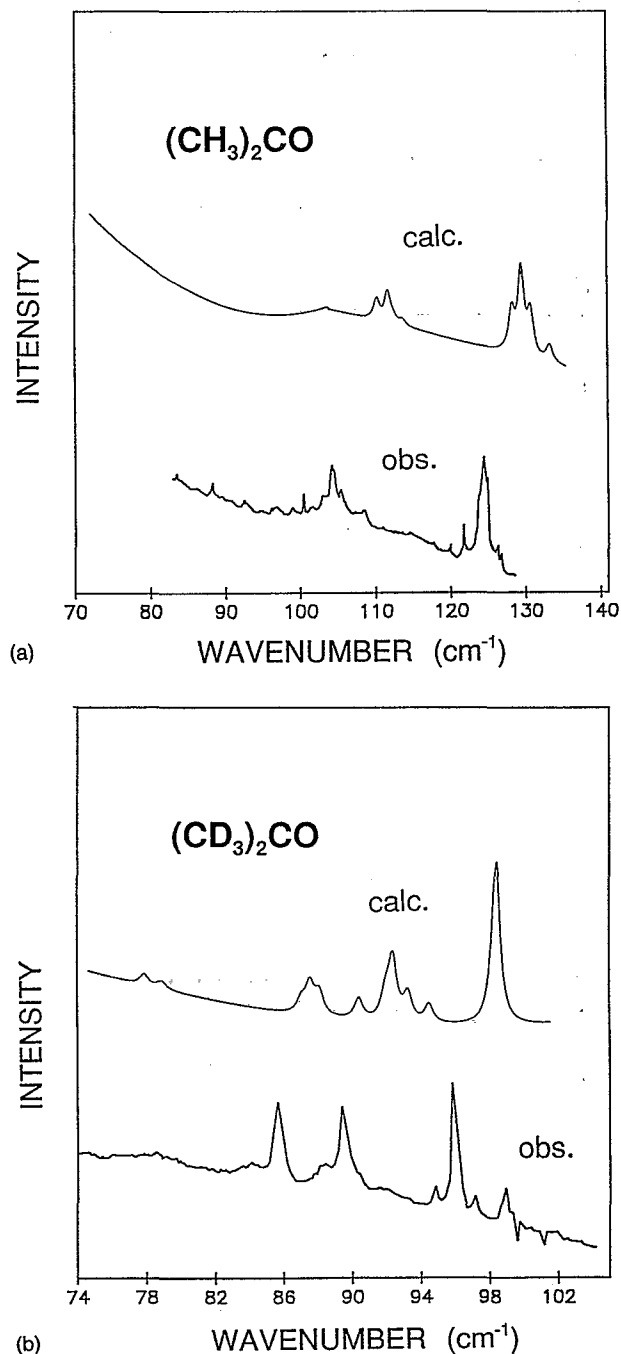calculated to have a more spread out structure. The multiplet structure increases to 3.38 cm^{-1}, and the ordering of the transitions is found to reverse: $E_1\to E_1$, 113.699 cm^{-1} (0.0678×10^{-4}), $E_4\to E_3$, 112.493 cm^{-1} (0.0596×10^{-4}), $G\to G$, 111.873 cm^{-1} (0.3271×10^{-4}), and $A_2\to A_1$, 110.320 (0.222×10^{-4}). Thus the ν_{17} first sequence would consist of four bands. The strongest band at 104.20 cm^{-1} is assigned to the $G\to G$ transition, the well defined component at 105.44 cm^{-1} to the pairs $E_1\to E_1$ and $E_4\to E_3$ and the low frequency band at 102.92 cm^{-1} to the $A_2\to A_1$ transition.

The band which could be assigned to the second se-

TABLE X. (A) The far infrared intensities and frequencies for acetone-h_6, variable kinetic energy parameters. (B) The far infrared intensities and frequencies for acetone-d_6, variable kinetic energy parameters.

(A) Acetone-h_6 Assign.[a] $v\ v' \to v\ v'$	MP2/RHF Freq.	Intensities	RHF Freq.	Intensities
0 0 0 1				
$A_1 \to A_2$	130.673	0.4705	128.919	0.4395
$G \to G$	129.447	0.9044	127.258	0.8314
$E_1 \to E_1$	128.489	0.2185	125.852	0.1977
$E_3 \to E_4$	128.474	0.2184	125.842	0.1977
0 1 0 2				
$A_2 \to A_1$	110.320	0.2220	104.838	0.1820
$G \to G$	111.873	0.3271	105.438	0.2133
$E_1 \to E_1$	113.699	0.0678	107.444	0.0435
$E_4 \to E_3$	112.493	0.0596	105.432	0.0360
0 2 0 3				
$A_1 \to A_2$	119.529	0.1720	118.254	0.1516
$G \to G$	139.143	0.0940	137.921	0.0302
$E_1 \to E_1$	143.229	0.0081	141.726	0.0003
$E_3 \to E_4$	144.895	0.0100	143.857	0.0002
2 0 2 1				
$A_1 \to A_2$	117.005	0.0415	117.666	0.0374
$G \to G$	109.496	0.0166	108.541	0.0099
$E_1 \to E_1$	84.595	0.0036	86.833	0.0024
$E_3 \to E_4$	75.357	0.0061	73.882	0.0054
1 0 1 1				
$A_3 \to A_4$	98.983	0.0807	94.758	0.0682
$G \to G$	106.160	0.1806	103.176	0.1550
$E_2 \to E_2$	111.396	0.0581	109.004	0.0517
$E_3 \to E_4$	111.705	0.0588	109.559	0.0529
(B) Acetone-d_6				
0 0 0 1				
$A_1 \to A_2$	98.648	0.2735	97.401	0.2544
$G \to G$	98.589	0.7934	97.307	0.7367
$E_1 \to E_1$	98.932	0.2907	97.583	0.2693
$E_3 \to E_4$	98.926	0.2907	97.575	0.2692
0 1 0 2				
$A_2 \to A_1$	92.304	0.2442	89.200	0.2082
$G \to G$	92.792	0.6393	90.625	0.5925
$E_1 \to E_1$	93.746	0.2643	90.426	0.1565
$E_4 \to E_3$	92.453	0.0955	92.316	0.2428
0 2 0 3				
$A_1 \to A_2$	90.759	0.1980	89.385	0.1802
$G \to G$	86.203	0.2086	80.601	0.0797
$E_1 \to E_1$	82.335	0.0564	77.603	0.0129
$E_3 \to E_4$	87.080	0.0704	81.048	0.0604
2 0 2 1				
$A_1 \to A_2$	80.938	0.0442	80.054	0.0414
$G \to G$	78.168	0.1065	76.639	0.0929
$E_1 \to E_1$	75.520	0.0353	74.367	0.0217
$E_3 \to E_4$	75.131	0.0353	72.728	0.0310
1 0 1 1				
$A_3 \to A_4$	87.302	0.1023	85.339	0.0917
$G \to G$	87.768	0.3038	86.008	0.2749
$E_2 \to E_2$	88.493	0.1138	86.907	0.1039
$E_3 \to E_4$	88.500	0.1138	86.913	0.1040

[a] v and v' are the vibrational quantum numbers.

quence is calculated to have its components in the following locations: $A_1 \to A_2$, 119.529 cm^{-1} (0.172$\times 10^{-4}$), $G \to G$, 139.143 cm^{-1} (0.0940$\times 10^{-4}$), $E_1 \to E_1$, 143.229 cm^{-1} (0.0081$\times 10^{-4}$) and $E_3 \to E_4$, 144.895 cm^{-1} (0.0100 $\times 10^{-4}$). The width of the torsional multiplet here is a result of the upper levels lying above the saddle point. Here the centrifugal distorsions could be expected to be more

important. These transitions cannot be located with certainty in the spectrum.

A number of weak peaks are observed, which may be attributed to cross sequence transitions. These transitions take place between the $\nu_{12}(a_2) + \nu_{17}(b_1)$ and $\nu_{12}(a_2)$ levels which are allowed by the $A_3 \to A_4$ selection rule. They are predicted to yield two sets of band clusters. The first cross

sequence transition results in the cluster: $A_3 \to A_4$, 98.983 cm^{-1} (0.0807×10^{-4}), $G \to G$, 106.160 cm^{-1} (0.1806×10^{-4}), $E_2 \to E_2$, 111.396 cm^{-1} (0.0581×10^{-4}), and $E_3 \to E_4$, 111.705 cm^{-1} (0.0588×10^{-4}). The weak band observed at 96.62 cm^{-1} is given the assignment $A_3 \to A_4$. The stronger $G \to G$ component is believed to be buried beneath the 111 cm^{-1} cluster of the first sequence transition. The $E \to E$ components are too weak to be observed.

It is interesting to note that the order of the first and second cross sequence transitions is reversed with respect to the fundamental and the first sequence transitions. The weak linelike features which are observed in this region of the spectrum probably result from water impurities in the sample. The problem of distinguishing acetone bands from water vapour lines prevents the weaker absorptions from being cataloged and assigned.

While not as extensive as the acetone-h_6 spectrum, the acetone-d_6 spectrum contains more bands and appears to be somewhat better resolved. Again, it is the degenerate $G \to G$ series of bands which dominate the spectrum. The fundamental, $v=0(G) \to v=1(G)$, is calculated to lie at 98.589 cm^{-1}, as the strongest band in the spectrum, intensity$=0.7934 \times 10^{-4}$. The calculated values for the three other components are $A_1 \to A_2$, 98.648 cm^{-1} (0.2735×10^{-4}), $E_1 \to E_1$, 98.932 cm^{-1} (0.2907×10^{-4}), and $E_3 \to E_4$, 98.926 cm^{-1} (0.2907×10^{-4}). The effect of the deuteration on the spectrum of acetone is to lower the levels within the potential well to the extent that the torsional cluster collapses together with a line width of 0.34 cm^{-1}. Collectively, these form a single band which is observed at 95.95 cm^{-1}.

The first sequence is calculated to be $E_4 \to E_3$, 92.453 cm^{-1} (0.0955×10^{-4}), $E_1 \to E_1$, 93.746 cm^{-1} (0.2643), $G \to G$, 92.792 cm^{-1}, and $A_2 \to A_1$, 92.304 cm^{-1} (0.2442×10^{-4}). As in acetone-h_6, the ordering of the components is reversed to that of the fundamental. The band at 89.41 cm^{-1} is assigned to the unresolved components $G \to G$ and $A_2 \to A_1$.

The second sequence is observed as a strong band at 85.65 cm^{-1} which does not appear to have torsional structure. From the calculated values: $A_1 \to A_2$, 90.759 cm^{-1} (0.1980×10^{-4}), $G \to G$, 86.203 cm^{-1} (0.2086×10^{-4}), $E_1 \to E_1$, 82.335 cm^{-1} (0.0564), and $E_3 \to E_4$, 87.080 cm^{-1} (0.0704×10^{-4}), the 85.65 cm^{-1} band could be assigned to the $A_1 \to A_2$ transition. The $G \to G$ transition seems to be buried under impurity absorption. The cross sequence transition, $A_3 \to A_4$ is calculated to lie at 87.302 cm^{-1} (0.1023×10^{-4}). This region of the spectrum contains many impurity interferences and additional assignments cannot be given.

Some experimental data is available for $v_{12}(a_2)$, the normal mode which comes from the clockwise–clockwise rotation of the two methyl groups. This mode is not active in the infrared as it transforms as a rotation rather than a translation. It should, however, be active in the Raman spectrum. The v_{12} fundamental has not been observed directly in the Raman spectrum of acetone vapor because of the weakness of the transitions. Harris and Levin[12] did observe a satellite band built on the side of the in-plane

TABLE XI. The observed and calculated torsional transitions for acetone-h_6 and -d_6 with the MP2/RHF potential energy function and variable kinetic parameters.[a,b]

	(CH$_3$)$_2$CO		(CD$_3$)$_2$CO	
	Calc.	Obs.	Calc.	Obs.
Mode v_{17} (clockwise–counterclockwise rotation)				
$v=0 \to v=1$				
$A_1 \to A_2$	130.67	125.16	98.65	
$G \to G$	129.45	124.61	98.59	95.95
$E_1 \to E_1$	128.49	123.90	98.93	
$E_3 \to E_4$	128.47	123.90	98.93	
$v=1 \to v=2$				
$A_2 \to A_1$	110.32	102.90	92.30	
$G \to G$	111.87	104.20	92.79	89.41
$E_1 \to E_1$	113.70	105.44	93.75	
$E_4 \to E_3$	112.49	105.44	92.45	
$v=2 \to v=3$				
$A_1 \to A_2$	119.53	108.55	90.76	85.63
Mode v_{12} (clockwise–clockwise rotation)				
$v=0 \to v=1$				
$A_1 \to A_3$	84.09	77.0[c]	58.13	55.0[c]
$v=1 \to v=2$				
$A_3 \to A_1$	89.27	85.0[c]	66.34	62.0[c]

[a]Basis set employed: 6–31G (d,p).
[b]Measured from Ref. 11, Fig. 1.
[c]From hot band intervals in the $n \to 3p_x$ Rydberg spectrum.

CCC bending mode which they attributed to a torsional–vibration combination band involving v_{12}. Recently Philis, Berman, and Goodman[15] have been able to observe v_{12} as a hot band frequency interval in the two-photon resonant multiphoton ionization spectrum of acetone. In the two photon process the selection rules allow the $^1A_1$ ground electronic state to combine with the Rydberg $^1A_2(n,3p_X)$ electronic state. For the acetone-h_6 isotopomer, they observed this interval to be 77 cm^{-1}, which is to be compared to our calculated value of 78.54 or 83.56 cm^{-1} in the RHF and MP2/RHF approximations. The overtone calculated at 166.55 or 175.15 cm^{-1} agrees nicely with the 162 cm^{-1} observed interval. In acetone-d_6 the agreement is found to be equally good. Observed and experimental data for acetone-h_6 and -d_6 are collected together in Table XI.

DISCUSSION

The potential surface illustrated in Fig. 3 is a $-60°$ to $+60°$ segment of the egg box potential, which for a complete rotation of the methyl groups, contains nine minima. In the region of the equilibrium position, the isoenergetic contour lines are oblong rather than circular as a result of the relatively large sine–sine gearing term. In the case of the $v_{17}(b_1)$ torsion, the normal mode tracks in the $\Theta_1 = \Theta_2$ direction which rises at 45° from the equilibrium position. The MP2/RHF energy at $\Theta_1 = +30°$, $\Theta_2 = +90°$ of 412.84 cm^{-1} is to be compared with $\Theta_1 = +30°$, $\Theta_2 = +30°$ of 252.34 cm^{-1} which is the equivalent point for torsional motion in the $v_{12}(a_2)$ direction. Both of these one dimensional slices out of the energy surface have identical barriers at $\Theta_1 = +60°$, $\Theta_2 = +60°$ of 793.62 cm^{-1}. Thus, the potential for torsion along the b_1 diagonal is narrower with steeper walls and can be described as V shaped. In the

other direction, the potential function is U shaped with a flatter bottom. Figure 4 shows the slices out of the potential surface in these two directions. The fundamental and the first overtone frequencies of the torsional modes are a reflection of these one dimensional potentials. For the b_1 mode, the A_1–A_2–A_1 MP2/RHF level separations display positive anharmonicity 130.673/110.320 cm^{-1}, while for the a_2 mode the A_1–A_3–A_1 anharmonicity is reversed, 84.087/89.267 cm^{-1}.

The MP2/RHF calculations with the 6–31G(p,d) basis were found to yield simulated far infrared spectra of acetone-h_6 and acetone-d_6 which adequately reproduce the observed spectra, Figs. 7(a) and 7(b). The calculated torsional energy levels are similar to those of Philis, Berman and Goodman,[15] who used identical electronic basis sets, but different grid points to define the potential surface. In all of the calculations, the torsional frequencies are calculated to be higher than the observed frequencies. Compare the MP2/RHF ν_{17} $v=0(A_1) \rightarrow v=1(A_2)$ fundamental for acetone-h_6 at 130.673 cm^{-1} with the corresponding observed value of 125.16 cm^{-1}. Neglecting the second order Möller–Plesset corrections for electronic correlation, RHF, move the calculated frequencies to better values, ν_{17}(RHF) = 128.919 cm^{-1}.

Introduction of the variable kinetic parameters caused the levels to fall in the correct direction. Table VIII(A) shows that for the MP2 approximation, the $v=1(A_2)$ level drops from 239.807 to 239.540 cm^{-1} with the introduction of variable kinetic terms. This correction, however, leads to only a small improvement in the fundamental frequency, 130.673 cm^{-1}, and does not offset the difference between the calculated and observed levels. Thus the present results show that the potential energy surfaces generated by the *ab initio* method are too rough, i.e., the barriers and saddle points to methyl torsion are too high. Corrections for electron correlation have the effect of making the surfaces even more undulating.

Now, the reasons for this mismatching have to be asked. The defect could be attributed to the inadequacy of the *ab initio* procedures (because of the truncated basis or the limited perturbation theory expansion employed). The RHF calculations, however, and especially the MP2/RHF ones reproduce well the locations of the lowest microwave levels.[4]

It is then reasonable to believe that the mismatching of the present calculation must come from the assumption that the torsional modes are independent of the other vibrational modes in the molecule. The CCCO squeleton of acetone is indeed known to be flexible. A coupling[14] between either the ν_8 a_1 in-plane CCC bending mode at 385 cm^{-1} or the ν_{16} b_1 out-of-plane C=O wagging mode at 484 cm^{-1} would have the effect of pushing the torsional levels downwards and compress them. In particular, the first excited out-of-plane wagging level, which is antisymmetric with respect to the molecular plane, may interact with any close A_2 torsional level.

The CCC group is seen to be flexible and, as Table IV shows, the CCC angle varies from 116.38° for the eclipsed–eclipsed conformation to 119.44° when the methyl groups

rotate by 60° to the staggered–staggered conformation. This flexing of the CCC with the rotation is a direct result of a steric crowding of the in-plane hydrogen atoms which point towards each other in the $\Theta_1 = 60°$, $\Theta_2 = 60°$ conformation. Some of these interactions are taken into account by optimizing the molecular structure at each conformation, which defines the potential energy surface. For a better description of the torsional modes, it would be necessary to extend the present model to include the flexing of the CCC angle, as well as the wagging angle of the carbonyl group, as additional large amplitude internal coordinates.

The intensities of the far infrared bands which result from internal rotation of the methyl groups are weak. It is the rotational contours of the bands with their strong central Q branch which allows the bands to be observed against the rising background absorption continuum. The spectra of the two isotopomers contain somewhat different information. In the case of acetone-h_6, the level splitting brought about by torsional nonrigidity is sufficiently large that clustering can be observed in the band assigned to the ν_{17} fundamental. This band is calculated to be the result of the four transitions $A_1 \rightarrow A_2$, 130.673 cm^{-1} (0.4705 $\times 10^{-4}$); $G \rightarrow G$, 129.447 cm^{-1} (0.9044 $\times 10^{-4}$); $E_1 \rightarrow E_1$, 128.489 cm^{-1} (0.2185 $\times 10^{-4}$); $E_3 \rightarrow E_4$, 128.474 cm^{-1} (0.2184 $\times 10^{-4}$). Thus the band attributed to the ν_{17} fundamental would consist of four overlapping subbands. It is the ratio of the statistical weights between the torsional microstates, which accounts for the calculated intensities. In the case of acetone-d_6, the level spitting is not observed, but three sequences can be clearly detected.

CONCLUSIONS

Acetone with its C_{2V} rigid frame and its C_{3v} methyl rotors may be regarded as a prototype system for studying the effects of strongly coupled large amplitude motion. The high symmetry of the G_{36} nonrigid group allows for the symmetry classification of the energy levels and the wave functions into nine representations and provides for a spectroscopic labelling of the infrared transitions.

In this paper, the far infrared torsional spectra of $(CH_3)_2CO$ and $(CD_3)_2CO$ molecules have been synthesized. For this purpose, the torsional frequencies were calculated from sophisticated *ab initio* calculations, and the intensities determined for the first time from the electric moment variations and the nuclear statistical weights. A correlation between the calculated and experimental spectra has allowed for an assignment of the major bands.

Another redeeming feature of the acetone system is that the saddle points and the tops of the barrier are at sufficiently low energies that the splitting of the torsional levels by the nonrigid motions of the methyl groups can be clearly observed in the acetone-h_6 far infrared spectrum. In this paper, the multiplet structures which results from the transitions between torsional microstates have been well reproduced when compared with the *available* experimental data.

The $v=0(A_1) \rightarrow v=1(A_2)$ frequency calculated with the MP2/RHF potential energy function of 130.673 cm^{-1}

is found to be slightly too high when compared with 125.16 cm^{-1} the experimental value. Thus the height of the barriers which controls the torsional frequencies is calculated to be too high. The correction for electron correlation has the effect of increasing the mismatch between the observed and calculated frequencies. The introduction of the variable internal rotational constant does adjust the frequencies in the downwards direction, but the improvement is very small.

A likely reason for the differences between the calculated and the observed frequencies could come from the assumptions made in the calculations. The model assumes that, while the torsional modes couple strongly with each other, they do not interact with the other modes in the molecule. The CCCO molecular frame of acetone undergoes skeletal vibrations. Two of them are of relatively low frequencies and can couple with the torsional modes. Interactions by either of these frame modes with the methyl tops would push and compress the torsional levels downwards and could account for the differences between the observed and calculated frequencies.

ACKNOWLEDGMENTS

[1] P. Groner, J. F. Sullivan, and J. R. Durig, in *Vibrational Spectra and Structure*, edited by J. R. Durig (Elsevier, New York, 1981), Vol. 9, p. 405.

[2] Y. G. Smeyers and M. N. Bellido, Int. J. Quantum Chem. **19**, 553 (1981).

[3] Y. G. Smeyers, A. Niño, and D. C. Moule, J. Chem. Phys. **93**, 5786 (1990).

[4] J. D. Swalen and C. C. Costain, J. Chem. Phys. **31**, 1562 (1959).

[5] R. Peter and H. Dreizler, Z. Naturforsch. Teil. A **20**, 301 (1965).

[6] R. Nelson and L. Pierce, J. Mol. Spectrosc. **18**, 344 (1965).

[7] T. Iijima, Bull. Chem. Soc. Jpn. **45**, 3526 (1972).

[8] J, M. Vacherand, B. P. Eijck, J. Burie, and J. Demaison, J. Mol., Spectrosc. **118**, 355 (1986).

[9] W. G. Fateley and F. A. Miller, Spectrochim. Acta **18**, 977 (1962).

[10] D. R. Smith, B. K. McKenna, and K. D. Moller, J. Chem., Phys. **45**, 1904 (1966).

[11] P. Groner, G. A. Guirgis, and J. R. Durig, J. Chem. Phys. **86**, 565 (1987).

[12] W. C. Harris and I. W. Levin, J. Mol. Spectrosc. **43**, 117 (1972).

[13] G. Dellepiane and J. Overend, Spectrochim. Acta **22**, 593 (1966).

[14] H. Hollenstein and H. H. Günthard, J. Mol. Spectrosc. **84**, 457 (1980).

[15] J. G. Philis, J. M. Berman, and L. Goodman, Chem. Phys. Lett. **167**, 16 (1990).

[16] (a) M. H. Whangbo and S. Wolfe, Can. J. Chem. **55**, 2778 (1977); (b) D. Cremer, J. S. Brinkley, J. Pople, and W. J. Hehre, J. Am. Chem. Soc. **96**, 6900 (1974); (c) P. Bowers and L. Schäfer, J. Mol. Struct. **69**, 233 (1980); (d) L. Radom, J. Baker, P. M. Gill, R. H. Nobes, and N. V. Riggs, *Ibid.* **126**, 271 (1985).

[17] Y. G. Smeyers, J. Mol. Struct. (Theochem) **107**, 3 (1984).

[18] J. K. G. Watson, Can. J. Phys. **43**, 1996 (1965).

[19] Y. G. Smeyers and M. N. Bellido, Int. J. Quantum Chem. **23**, 107 (1983).

[20] Y. G. Smeyers and A. Huertas-Cabrera, Theor. Chim. Acta **64**, 97 (1983).

[21] J. S. Crighton and S. Bell, J. Mol. Spectrosc. **118**, 383 (1986).

[22] A. G. Ozkabak, J. G. Philis, and L. Goodman, J. Am. Chem. Soc. **112**, 7854 (1990).

[23] A. G. Ozkabak and L. Goodman, Chem Phys. Lett. **176**, 19 (1991).

[24] M. A. Harthcock and J. Laane, J. Phys. Chem. **89**, 4231 (1985).

[25] (a) Y. G. Smeyers, *Memorias*, Vol. 13 (Real Academia de Ciencias, Madrid, 1989); (b) Y. G. Smeyers, Fol. Chim. Theor. Lat. **17**, 73 (1989); (c) Y. G. Smeyers, *Advances in Quantum Chemistry* (Academic, New York, 1992), Vol. 24, pp. 1–77.

[26] Y. G. Smeyers and A. Hernández-Laguna, *Structure and Dynamics of Molecular Systems* (Reidel, New York, 1985), Vol. 40.

[27] H. C. Longuet-Higgins, Mol. Phys. **6**, 445 (1963).

[28] J. Maruani, Y. G. Smeyers, and A. Hernández-Laguna, J. Chem. Phys. **76**, 3123 (1982).

[29] Y. G. Smeyers and A. Hernández-Laguna, Int. J. Quantum Chem. **22**, 681 (1982).

[30] E. B. Wilson, Jr., J. Chem. Phys. **3**, 276 (1935).

[31] Y. G. Smeyers and A. Niño, J. Comp. Chem. **8**, 330 (1987).

[32] R. H. Judge, Comput. Phys. Commun. **47**, 361 (1987).

[33] M. L. Senent, Ph.D. thesis, University of Valladolid, Valladolid, Spain, 1992.